



The differences in geometry modifications methods after topological optimization

Jiri Struz¹  and Lukas Hruzik² 

^{1,2} Department of machine parts and mechanisms, VSB – TU Ostrava, 17. listopadu 2172/15,
708 00 Ostrava, Czech Republic
jiri.struz@vsb.cz

Abstract. The presented article compares two types of software in terms of the post-processing of topological optimization. For this analysis, a test sample was selected and subjected to topological optimization concerning weight reduction while ensuring maximum rigidity. Subsequently, the sample was processed using two modules that the individual software contains. During the post-processing phase, surface smoothing options, elements of bionic structure and standard remodelling tools were used. The results obtained were compared in terms of weight achieved. Based on the analysis, it was found that post-processing requiring manual modifications done by a designer show greater weight than in the case of smoothing provided by the software. The approaches of the individual software were also compared in terms of the creation of a finite element network for both static analysis and topological optimization. It was found that in the case of one software, the finite element network is background modified before the topological optimization starts.

Keywords: Topology optimization; Design region; Weight reduction, 3D printing.

1 Introduction

In recent years, topological optimization has experienced a very rapid boom in the field of machine parts design due to the development of 3D printing. The principle of topological optimization is generally based on special optimization, material distribution or maximization, or the minimization of target parameters. [1] These parameters can also be analysed using different approaches. For example, [2], [3], [4] deal with topological optimization focused on harmonic frequency in terms of deformations, acceleration or their combination. The results may be influenced by the selection of the calculation method, which is described in [5], where at the end of the process the weights of the samples, as well as the difference between the stresses, are compared. A comparison of deformation models is discussed by [6], which offers a comparison of three lattice structure types. In addition, it also investigates mechanical properties and the ability to absorb energy. The research has shown that the VC lattice is stronger than the FCC and ECC concerning the stress in violation.

As indicated above, a frequent calculation criterion is weight reduction while maintaining maximum stiffness. Jeong [7] describes the criterion of an increase in stiffness.

© The Author(s) 2024

M. Petr et al. (eds.), *62nd International Conference of Machine Design Departments (ICMD 2022)*,

Atlantis Highlights in Engineering 28,

https://doi.org/10.2991/978-94-6463-423-5_32

Other optimized parameters can be shape, area, and parameters in terms of dynamics [8], [9], [10], hydrodynamics and flow. [11]

Another rather comprehensive topic is the optimization of structures with cracks, the goal of which is to eliminate potential defects at the design stage. For example, [12] compared the FEM and peridynamic approaches. It states that the peridynamic approach provides better support for the notched structures, while the deformation energy is much lower than with the use of the FEM approach.

2 Methodology

The methodology consists of defining a geometric-shaped sample on which individual post-processing procedures will be applied. In addition, the sample will be subjected to static analysis which is a necessary pre-stage for topological optimization. Based on the results of the static analysis, topological optimization will be carried out, where design and exclusion regions will be defined as the given software allows it. After topological optimization is performed, the results of the masses will be compared above all. The methodology schematic diagram can be seen in **Fig. 1**.



Fig. 1. Methodology schematic diagram

The sample on which the analysis will be done is displayed in **Fig. 2**, while the boundary conditions with the load force of 2,000N are also defined.

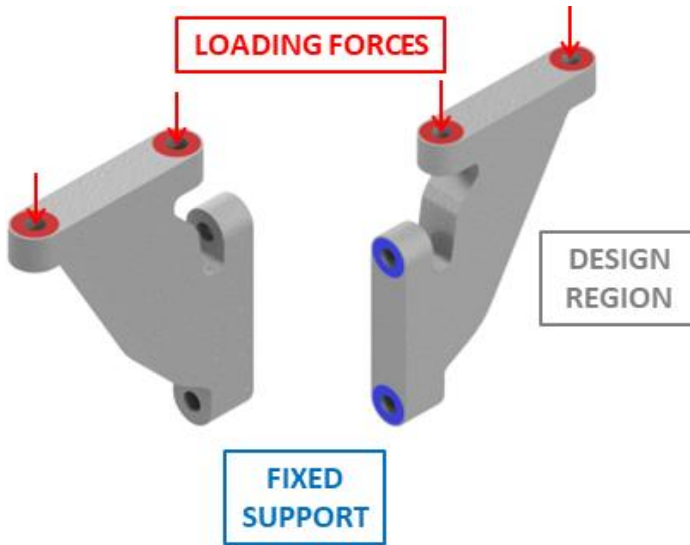


Fig. 2. Boundary conditions definition

2.1 Software options

Ansys Workbench and Altair Inspire software were used in this comparative study. Each of them allows us to provide topological optimization in different ways, as well as work with the resulting geometry. In the case of Ansys Workbench software, we can choose from the following calculation methods:

- Topology optimization – Density based
- Lattice optimization
- Topology optimization – Level set based
- Topology optimization – Morphing

The calculation criteria for these two softwares are listed in **Table 1**.

Table 1. Overview of criteria definition options

Criterion	Ansys Workbench	Altair Inspire
Maximum stiffness while reducing weight	+	+
Minimising displacement	+	
Minimisation of mass	+	+
Minimisation of volume	+	
Minimisation of reaction force	+	
Centre of gravity	+	
Moment of inertia		
Global von Mises stress	+	

Local von Mises stress	+	
Criterion	+	
Maximum frequency		+

It should be noted here that Altair Inspire software allows us to set, in addition to the standard criterion of maximum stiffness while reducing weight, also the following limitations:

- Maximum frequency
- A definition of the minimum frequency

Other differences can be found in the post-processing options. Altair Inspire excels in the possibility of creating bionic structures using the PolyNURBS module. Using this module, we can also provide the standard smoothing – selecting the “smooth” option. Another option available is the possibility to modify the geometry by a standard manual operation, the so-called remodelling. Ansys Workbench also offers similar tools. However, it does not allow us to create bionic structures. Thus, the final model modification is then limited to smoothing and remodelling.

In this study, we will use the above-stated capabilities of each software and compare the resulting weights. When comparing them, the resulting shapes and their proper functionality will also be taken into account.

3 Topology optimization

Based on the boundary conditions defined in **Fig. 2**, static analysis was performed first. The aim of this study is to compare the weight results depending on the post-processing method used, as well as the differences between the individual softwares. For this reason, individual commands were entered possibly for the same values to get a better picture of how each software works. One of them is the finite element network. Within this analysis, the defined size of the element was 6mm. Material parameters were also considered to be identical. An overview of the number of elements and nodes is displayed in **Table 2**. This overview shows that Altair Inspire software will regenerate the network in the background of the calculation provided for topological optimization, changing the ratio of nodes and elements.

Table 2. Number of elements and nodes

	Ansys SA	Ansys TO	Inspire SA	Inspire TO
Elements	18176	18176	10480	109877
Nodes	27823	27823	18084	21370

Gi-Static Structural
 Equivalent Stress
 Type: Equivalent (von-Mises) Stress
 Units: MPa
 Time: 1
 24.09.2022 10:53
 12.730 Max
 11.317
 9.9156
 8.5208
 7.0951
 5.6803
 4.2665
 2.8567
 1.443
 0.033208 Min

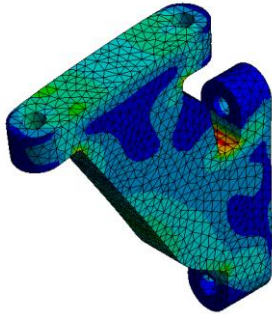


Fig. 3. Results from static analysis from Ansys – von Mises stress

Gi-Static Structural
 Directional Deformation
 Type: Directional Deformation(Y Axis)
 Units: mm
 Global Coordinate System
 Time: 1
 24.09.2022 10:54
 0.00020619 Max
 -0.0016743
 -0.0050488
 -0.0054233
 -0.0072976
 -0.0091722
 -0.011047
 -0.012791
 -0.014796
 -0.01667 Min

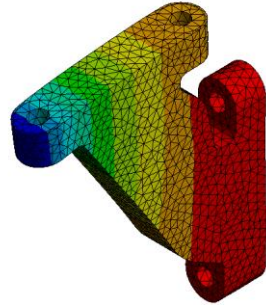
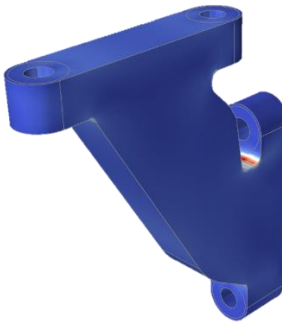
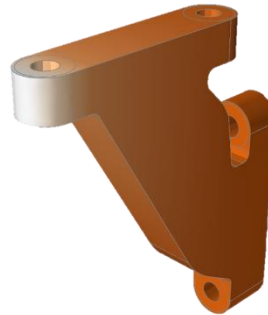


Fig. 4. Results from static analysis from Ansys – deformation in the load direction



Max: 1.552e+01 MPa
 — 1.552e+01 MPa
 — 1.397e+01 MPa
 — 1.242e+01 MPa
 — 1.087e+01 MPa
 — 9.321e+00 MPa
 — 7.772e+00 MPa
 — 6.223e+00 MPa
 — 4.675e+00 MPa
 — 3.126e+00 MPa
 — 1.577e+00 MPa
 — 2.864e-02 MPa
 Min: 2.864e-02 MPa

Fig. 5. Results from static analysis from Altair Inspire – von Mises stress



Max: 1.936e-04 mm
 — 1.936e-04 mm
 — -1.467e-03 mm
 — -3.127e-03 mm
 — -4.788e-03 mm
 — -6.448e-03 mm
 — -8.108e-03 mm
 — -9.769e-03 mm
 — -1.143e-02 mm
 — -1.309e-02 mm
 — -1.475e-02 mm
 — -1.641e-02 mm
 Min: -1.641e-02 mm

Fig. 6. Results from static analysis from Ansys – deformation in the load direction

From the picture shown above, it can be seen that Altair Inspire states a maximum stress of 15.5 MPa and deformation of 0.01641 mm. The maximum stress is noticeable in **Fig. 5** at the point of the shape transition. In contrast, Ansys software has a maximum stress value of 12.7 MPa and maximum deformation of 0.01664 mm. The maximum stress and deformation can be found in the same areas as in the previous case.

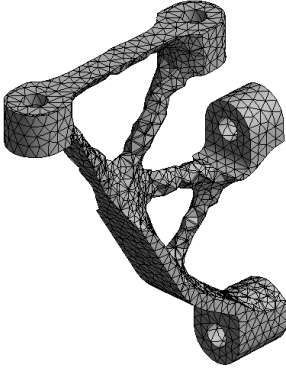
Table 3. Comparison of static analysis results

	Ansys	Altair Inspire
von Mises stress [MPa]	12.7	15.5
Deformation Y [mm]	0.01664	0.01641

The following figures display the results of topological optimization. In the case of Ansys Workbench software, a topological optimization method called “Level set based“ was selected. The target weight in both cases was considered to be lower than the original one by 70 %. The result can be found in **Fig. 6**. The resulting weights obtained by each software are listed in **Table 4**.

Table 4. Weights of topological optimization results [kg]

	Ansys	Altair Inspire
Mass	1.007	1.264

**Fig. 7.** Results of topology optimization in Ansys**Fig. 8.** Results of topology optimization in Altair Inspire with partitions – **Altair Inspire 2**

4 Geometry modifications

After carrying out topological optimization, the obtained results were subjected to geometric modifications. In **Fig. 7**, the result of topological optimization in Ansys can be seen. Ansys has a “smooth” function, the result of which is evident in **Fig. 9 9**. By comparing these two figures, we can see that a significant smoothing of the surface has been provided. In contrast, **Fig. 10** displays the geometric modification of the result obtained by remodelling. This can be done quite easily in the SpaceClaim programme, which is part of the Ansys program and contains the above-mentioned function “smooth“. When remodelling, it is necessary to take into account the influence of the human factor. SpaceClaim can accurately project a section of geometries from topological optimization into a sketch. However, there are often some simplifications that can entail an emerging deviation from the original result.

Altair Inspire, on the other hand, allows for the creation of bionic structures using the PolyNURBS function. The result of this activity can be found in **Fig. 12**. The principle of this method is in interlacing of the geometry from topological optimization by the new bionic geometry. Basically, this is another kind of remodelling since the result is again influenced by the human factor. Modification obtained using the PolyNURBS Fit command is also worth mentioning, as this basically binds partitions with the design region. The geometry obtained is very similar to the geometry illustrated in **Fig. 911**.

One of the last options is to provide manual remodelling again. Use-friendliness for remodelling is significantly worse than in the case of Ansys software, which, on the contrary, is redeemed by the possibility of creating bionic structures. **Fig. 13** displays the result of the geometry obtained after smoothing. Here again, smoothing can be done together for partitions with the design region.

In conclusion, the great advantage of Altair Inspire software is its option to create bionic structures in several ways. Analyses can also be set up relatively easily. On the other hand, if a designer wanted to produce a model using conventional methods, its modification is not very user-friendly in an Altair Inspire environment. Nevertheless, it is not impossible to provide. From the use of the Ansys software, it can be deduced that it does not focus purely on 3D printing, but also on standard production methods. Although it does not have the option to create bionic structures, it allows us to perform the calculation of topological optimization by a number of methods. Also, editing the geometric result in the SpaceClaim environment is more user-friendly. Using **Fig. 9**, **Fig. 11** and **Fig. 13**, it can be concluded that Ansys, when the “Level set based“ method is used, creates a constant line at the top of the model compared to the Altair Inspire. On the other hand, Altair Inspire creates an open pocket in the central part. In the same place, Ansys forms a hole and connects the platforms for bolts using rods. The resulting weight from Ansys is 1.007kg versus 1.264kg in the case of Altair Inspire. The higher weight is mainly due to partitions, which Altair Inspire automatically treats as an excluded region, thus replacing the design region.

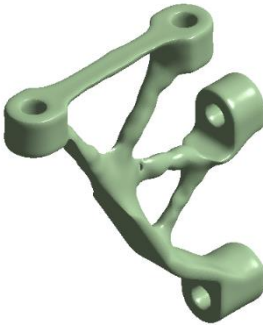


Fig. 9. Ansys Workbench model after smooth

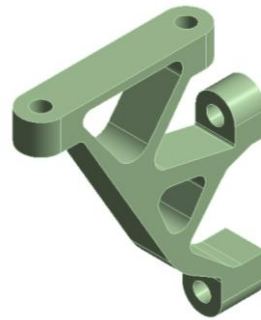


Fig. 10. Ansys Workbench model after remodelling



Fig. 11. Altair Inspire model after Poly-NURBS Fit



Fig. 12. Altair Inspire model after Poly-NURBS



Fig. 13. Altair Inspire model after smooth

Fig. 14. Altair Inspire model after remodelling

5 Discussion

Using the “smooth” command in the SpaceClaim program, which is a part of the Ansys program environment, the geometry displayed in **Fig. 9** was smoothed. The resulting weight after smoothing is 1.0506 kg, which represent an increase from the original weight by 4.2 %. In the case of remodelling (**Fig. 10**), the weight of 1.7013 kg was obtained, which is 40.8 % more than the original weight. However, the achieved weight was significantly influenced by the skills and abilities of the designer, which leads to a considerable individualization of the results. In the case of the Altair Inspire program, using the “smooth” function helped to reach a weight of 1.2491 kg. This means that the weight was reduced by 1.15 %. Using PolyNURBS Fit (**Fig. 11**), the weight was reduced to 1.098 kg from the starting 1.264 kg, which corresponds to a weight reduction of approximately 13 %. Conversely, using the PolyNURBS command the geometry obtained (**Fig. 12**) showed a weight of 1.3039 kg. This weight proves a slight increase by 3.2 %. Again, it is necessary to bear in mind that this weight is influenced by the skills and abilities of the designer to guide the rods of bionic structures. As in previous case, the geometry was manually remodelled again (**Fig. 14**). By remodelling, the weight of 1.6124 kg was achieved. This corresponds to an increase from the original weight by 27.6 %.

From the above, we can note that some methods lead to weight loss, and some, on the contrary, lead to its increase (**Fig. 15**). Interestingly, in the case of the “smooth” function, Ansys brings a slight increase in weight, while in the case of Altair Inspire, there is a slight decrease of weight. For methods that require manual remodelling (PolyNURBS and remodelling), there was an increase of weight in both cases. From

experience, this phenomenon always occurs, but it is influenced by the skills and experience of the designer.

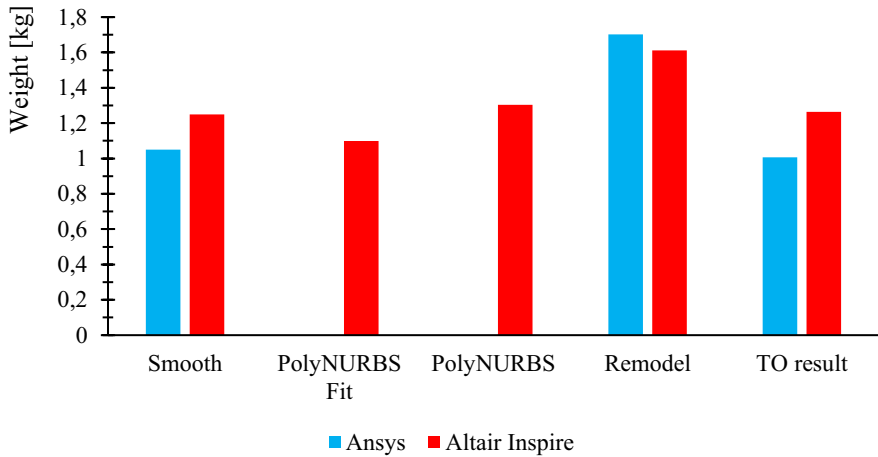


Fig. 15. Weight comparison

For all these analyses, the same values for individual commands were set as far as possible. The same element size value has been defined both in the creation of the finite elements network and in the smoothing process. The data prove that in Altair Inspire, the number of elements and nodes is adjusted in the background before topological optimization starts. At this point, it should also be noted that the results will be very individual depending on the examined geometry and abilities of the designer.

6 Conclusion

The article presents a study on the influence of post-processing methods on the resulting sample weight. In this case, it was found that the “smooth“ function endured the slightest change in weight. On the contrary, Altair Inspire decreases the weight. Ansys slightly increases the weight. Methods requiring designer modeling, on the other hand, cause weight gain in most cases, but the results will be very individual on a case-by-case basis. Remodelling in Ansys feels more user-friendly than on Altair Inspire. By contrast, its advantage is the possibility of creating bionic structures, leading to interesting design outcomes. It is also more suitable for 3D printing.

Acknowledgment

This article was developed within the project SP2022/10 – “Experimental and computational methods of machine parts dimensioning 2022“.

References

1. BENDSøE, Martin P. a Ole SIGMUND. *Topology Optimization Theory, Methods, and Applications*. 2nd ed. Germany: Springer Berlin Heidelberg, 2013. ISBN 3-540-429992-1.
2. LIU, Hu, Weihong ZHANG a Tong GAO. A comparative study of dynamic analysis methods for structural topology optimization under harmonic force excitations. *Structural and Multidisciplinary Optimization*. 2015, 51(6), 1321-1333. ISSN 1615-1488. Dostupné z: doi:10.1007/s00158-014-1218-4
3. BANKOTI, Saurabh, Akash DHIMAN a Anadi MISRA. Comparative Analysis of Different Topological Optimization Methods with ANSYS. *INTERNATIONAL JOURNAL FOR RESEARCH IN EMERGING SCIENCE AND TECHNOLOGY*. 2015, 2(4), 84-89. ISSN 2349-7610.
4. GUO, Jincheng a Huaping TANG. Stiffness-Oriented Structure Topology Optimization for Hinge-Free Compliant Mechanisms Design. 2021, . ISSN 2076-3417. Dostupné z: doi:10.3390/app112210831
5. TYFLOPOULOS, Evangelos a Martin STEINERT. Topology and Parametric Optimization-Based Design Processes for Lightweight Structures. 2020, . ISSN 2076-3417. Dostupné z: doi:10.3390/app10134496
6. YANG, Chengxing, Kai XU a Suchao XIE. Comparative Study on the Uniaxial Behaviour of Topology-Optimised and Crystal-Inspired Lattice Materials. 2020, . ISSN 2075-4701. Dostupné z: doi:10.3390/met10040491
7. JEONG, Gil-Eon. Topology Optimization of Deformable Bodies with Linear Dynamic Impact and Frictionless Contact Condition. 2021, . ISSN 2076-3417. Dostupné z: doi:10.3390/app112210518
8. MUNK, David J., Gareth A. VIO a Grant P. STEVEN. Aerothermoelastic Structural Topology Optimisation for a Hypersonic Transport Aircraft Wing. In: LI, Qing, Grant P. STEVEN a Zhongpu (Leo) ZHANG. *Aerothermoelastic Structural Topology Optimisation for a Hypersonic Transport Aircraft Wing: Proceedings of the 11th World Congress of Structural and Multidisciplinary Optimization (WCSMO-11)* [online]. Sydney, Australia, 2015, s. 31-36 [cit. 2022-06-30]. ISBN 978-0-646-94394-7.
9. IKEYA, Kenichi a Masatoshi SHIMODA. Multi-objective Free-form Optimization for Shape and Thickness of Shell Structures with Composite Materials. In: LI, Qing, Grant P. STEVEN a Zhongpu (Leo) ZHANG. *Advances in Structural and Multidisciplinary Optimization: Proceedings of the 11th World Congress of Structural and Multidisciplinary Optimization (WCSMO-11)*, June 7-12, 2015, Sydney, Australia [online]. Sydney, Australia, 2015, s. 231-236 [cit. 2022-06-30]. ISBN 978-0-646-94394-7.
10. CZARNECKI, Sławomir, Radosław CZUBACKI, Tomasz LEWINSKI a Paweł WAWRUCH. Topology optimization of continuum structures made of non-homogeneous materials of isotropic or cubic symmetry. In: LI, Qing, Grant P. STEVEN a Zhongpu (Leo) ZHANG. *Advances in Structural and Multidisciplinary Optimization: Proceedings of the 11th World Congress of Structural and Multidisciplinary Optimization (WCSMO-11)* [online]. Sydney, Australia, 2015, s. 83-88 [cit. 2022-06-30].
11. GHASEMI, Ali a Ali ELHAM. A Novel Topology Optimization Approach for Flow Power Loss Minimization Across Fin Arrays. 2020, . ISSN 1996-1073. Dostupné z: doi:10.3390/en13081987
12. LAHE MOTLAGH, Peyman a Adnan KEFAL. Comparative Study of Peridynamics and Finite Element Method for Practical Modeling of Cracks in Topology Optimization. 2021, . ISSN 2073-8994. Dostupné z: doi:10.3390/sym13081407

Open Access This chapter is licensed under the terms of the Creative Commons Attribution-NonCommercial 4.0 International License (<http://creativecommons.org/licenses/by-nc/4.0/>), which permits any noncommercial use, sharing, adaptation, distribution and reproduction in any medium or format, as long as you give appropriate credit to the original author(s) and the source, provide a link to the Creative Commons license and indicate if changes were made.

The images or other third party material in this chapter are included in the chapter's Creative Commons license, unless indicated otherwise in a credit line to the material. If material is not included in the chapter's Creative Commons license and your intended use is not permitted by statutory regulation or exceeds the permitted use, you will need to obtain permission directly from the copyright holder.

